Available online at www.sciencedirect.com
ScienceDirect
Journal of Power Sources 168 (2007) 493–500
JOURNAL OF POWER SOURCES
www.elsevier.com/locate/jpowsour

Characterization of electrode/electrolyte interface for lithium batteries using *in situ* synchrotron X-ray reflectometry—A new experimental technique for $LiCoO_2$ model electrode

Masaaki Hirayama [a], Noriyuki Sonoyama [a], Takeshi Abe [a], Machiko Minoura [a], Masumi Ito [a], Daisuke Mori [a], Atsuo Yamada [a], Ryoji Kanno [a,*], Takahito Terashima [b], Mikio Takano [b], Kazuhisa Tamura [c], Jun'ichiro Mizuki [c]

[a] *Department of Electronic Chemistry, Interdisciplinary Graduate School of Science and Engineering, Tokyo Institute of Technology, 4259 Nagatuta, Midori-ku, Yokohama 226-8502, Japan*
[b] *Institute of Chemical Research, Kyoto University, Uji, Kyoto-fu 611-0011, Japan*
[c] *Japan Atomic Energy Agency, Synchrotron Radiation Research Center, Kansai Research Establishment, 1-1-1 Kouto Sayo-cho Sayo-gun, Hyogo 679-5148, Japan*

Received 26 September 2006; received in revised form 6 March 2007; accepted 7 March 2007
Available online 19 March 2007

Abstract

A new experimental technique was developed for detecting structure changes at electrode/electrolyte interface of lithium cell using X-ray reflectometry and two-dimensional model electrodes with a restricted lattice-plane. The electrodes were constructed with an epitaxial film of $LiCoO_2$ synthesized by pulsed laser deposition method. The orientation of the epitaxial film depends on the substrate plane; the 2D layer of $LiCoO_2$ is parallel to the $SrTiO_3$ (1 1 1) substrate ($(0\,0\,3)_{LiCoO_2}//(1\,1\,1)_{SrTiO_3}$), while the 2D layer is perpendicular to the $SrTiO_3$ (1 1 0) substrate ($(1\,1\,0)_{LiCoO_2}//(1\,1\,0)_{SrTiO_3}$). The anisotropic properties were confirmed by electrochemical measurements. *Ex situ* X-ray reflectivity measurements indicated that the impurity layer existed on the as-grown $LiCoO_2$ was dissolved and a new SEI layer with lower density was formed after soaking into the electrolyte. *In situ* X-ray reflectivity measurements indicated that the surface roughness of the intercalation (1 1 0) plane increased with applying voltages, while no significant changes in surface morphology were observed for the intercalation non-active (0 0 3) plane during the pristine stage of the charge–discharge process.

Keywords: Epitaxial thin-film; Lithium battery; Electrode/electrolyte interface; Reflectivity

1. Introduction

Since the lithium-ion configuration composed of carbon anodes and intercalation cathodes has been widely accepted for lithium secondary batteries, significant efforts have been devoted to attain high energy and power densities to produce an excellent energy storage system [1]. In particular, recent progress in pure electric vehicles (EV) and hybrid electric vehicles (HEV) requires high power operation for the current battery systems. Power characteristics of the battery systems are closely related to the nature of electrode reaction, which is composed of several reaction steps proceeded in series: lithium diffusion in the electrolyte, adsorption of solvated lithium on the cathode surface, de-solvation, surface diffusion, charge-transfer reaction, intercalation from the surface to the bulk, and the bulk diffusion of lithium in the electrode material. Recent electrochemical studies have claimed that the de-solvation process was a rate-determining step of the whole electrode reaction [2,3].

It is well known that electrode surfaces are almost covered with a passive surface layer, which is generally called a solid electrolyte interface (SEI). The idea of the SEI layer was originally introduced on the alkali and alkaline earth metal in organic electrolytes [4], and it is believed that the layer plays a key role in the electrochemical performance, particularly the calendar life of lithium batteries. Many experimental techniques, such as XPS [5–8], infrared spectroscopy [9,10], NNR [11] and

* Corresponding author. Tel.: +81 459245401; fax: +81 459245401.
E-mail address: kanno@echem.titech.ac.jp (R. Kanno).

0378-7753/$ – see front matter © 2007 Elsevier B.V. All rights reserved.
doi:10.1016/j.jpowsour.2007.03.034

ellipsometry [12] have been employed to study the nature and formation mechanism of the SEI layer. However, the previous studies were based on polycrystalline materials, which contain the effects of many parameters; for example, surface structure, surface morphology, surface defect, grain boundary, and even a reaction between the electrode and electrolyte. The system might not be suitable for clarifying electrode reaction mechanism. The electrode reaction at the electrode/electrolyte interface of lithium batteries is still ambiguous, and a comprehensive understanding of the reaction is an important subject for promoting electrode reaction and for designing new electrode materials suitable for high power operation. However, there are very few experimental techniques which allow direct observation of the electrode/electrolyte interface during the electrochemical reactions.

X-ray reflectivity method is one of the best experimental techniques to detect the electrode surface during the electrochemical reactions. However, the electrode surface should be flat with a roughness of ∼1 nm, and it was only applied for ideal electrode system, such as under potential deposition (UPD) process [13–15]. Our approach is to clarify the reactions at the interface of the intercalation electrode of lithium batteries with developing new experimental setup for ideal two-dimensional electrodes for practical battery systems.

In the present study, we tried to design an ideal electrode suitable for investigating interfacial reactions at the two-dimensional electrode surface. The epitaxial thin-films of cathode material, $LiCoO_2$, were successfully synthesized on single crystal substrates, $SrTiO_3$. These films were characterized by thin-film X-ray diffraction (XRD) method, and their properties were determined by electrochemical measurements. The surface structures of the electrodes were characterized by the combined used of *ex situ* and *in situ* reflectivity measurements. The relationship between the surface reaction and the electrochemical property will be discussed.

2. Experimental

$LiCoO_2$ films were grown using a KrF excimer laser with a wavelength of 248 nm under O_2 and a pulsed laser deposition (PLD) apparatus, PLD 3000 (PVD products, Inc.). The substrate used was single crystals of Nb doped $SrTiO_3$ (10 mm × 10 mm × 5 mm size). The conductivity of the substrate was 5.28×10^{-3} Ω cm at room temperature. The orientations of the substrate crystals were (1 1 1), (1 1 0) and (1 0 0) for $SrTiO_3$. The targets for the PLD process were synthesized by sintering starting materials at high temperatures. Li_2CO_3 and Co_3O_4 were used for the starting materials. The target had an excess lithium composition (Li/Co = 1.0–1.3) to compensate a lithium loss during the PLD process. The lattice parameters of the targets were $a = 2.81468(3)$ and $c = 14.049(2)$ Å, which are consistent with the JCPDS (#350782) values of $a = 2.8166$ and $c = 14.052$ Å. For the PLD experiments, we changed the oxygen pressure, laser power, laser frequency, distance between target and substrate, substrate materials, and synthesis temperatures. The thin-film X-ray diffraction (XRD) data were recorded by a thin-film X-ray diffractometer, ATX-G (Rigaku) with Cu $K\alpha_1$ radiation. The orientation of the films were characterized both by the out-of-plane and in-plane technique. The incident angle was set at 0.1° in all in-plane measurements.

The charge–discharge characteristics of the epitaxial films deposited on the $SrTiO_3$ substrate were examined with a lithium cell using lithium metal as an anode. The cut-off voltages were 2 and 4.2 V, and the current of charge–discharge was set at 1 μA (approximately 0.5 C). The electrolyte used was EC (ethylene carbonate)–DEC (di-ethyl carbonate) with a molar ratio of 3:7 as a solvent and a supporting electrolyte of 1 M $LiPF_6$.

The surface structure change of the electrode was measured by *ex situ* X-ray reflectivity measurements using a thin-film X-ray diffractometer, ATX-G, after the film was soaked into the electrolyte or after the lithium cell was constructed. The surface change during the electrochemical reactions was observed by reflectivity measurements with an X-ray/electrochemical cell in the transmission geometry. The cell was mounted on the theta stage of a κ-type six-circle diffractometer (New Port) installed on a bending-magnet beamline BL14B1 at SPring-8. The X-rays were monochromated by a Si (1 1 1) double crystal system and focused by two Rh-coated bent mirrors. The beam size of the incident X-ray was 0.1 mm (vertical) × 0.4–1.0 mm (horizontal), which was adjusted by a slit placed in front of the sample. The angular acceptance of the receiving slit was 2 mrad for the 2θ direction and 20 mrad for the χ-direction. A wavelength of 0.399102 Å (31 keV) was selected for penetrating X-rays through the organic solvent used in the *in situ* electrochemical cell. The reaction was controlled by a potentiostatic method with a potentiostat/galvanostat (Hokuto Denko, HA-501). The cell voltage increased at an interval of about 0.2 or 0.5 V from the initial voltage to 4.0 V. Electrolyte solution of EC:DEC with 3:7 molar ratio with 1 M $LiPF_6$ was injected into the spectroelectrochemical cell. The reflectivity was measured after applying a fixed voltage. The cell voltage was fixed for 30–60 min in the *in situ* XRR measurements. Fig. 1 shows the newly designed

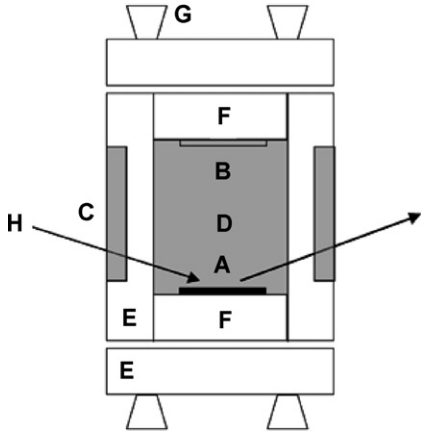

Fig. 1. Schematic diagram of the *in situ* electrochemical cell for X-ray reflectivity measurements. The window material is Mylar film, and the cell was constructed from stainless steel. The counter electrode was lithium metal. The ohmic contact between the substrate and the cell was obtained by Ga–In paste. The overall size of the cell was 58 mm × 58 mm × 52 mm (A, epitaxial film (10 mm × 10 mm); B, counter electrode (Li foil); C, Mylar film (percolation window); D, electrolyte; E, cell body (stainless); F, electrode folder; G, screw; H, X-ray).

spectroelectrochemical cell for *in situ* thin-film X-ray reflectivity measurements. The black closed part (A) is an epitaxial film with the substrate. The cell was equipped with a Li counter electrode (B). It was sealed with a 6.0 μm thick Mylar film (Chemplex, D), which served as an X-ray window. The body of the cell (E) and the holder of the sample (F) were made of stainless steel. All the measurements were carried out in such a mode that the incoming and outgoing angles with respect to the sample surface were equal. The reflectivity data were recorded for the angle range of 0–0.6°. The models of surface structure were refined by the Parratt32 data analysis program [16] with the reflectivity calculated using Parratt's method [17], using roughness, thickness and scattering length density (SLD) of each layer as parameters. The density of the layer, d, was estimated by real part of the SLD with the following equation.

$$d = \frac{M \times \mathrm{SLD}}{r_0 N_\mathrm{a} Z} \quad (1)$$

where M is the molecular weight, r_0 the Bohr atomic radius, N_a the Avogadro's number and Z is overall atomic weight.

3. Results and discussion

3.1. Synthesis and characterization of the epitaxial films

The synthesis conditions of the PLD method optimized were as follows: target composition, a molar ratio of Li/Co = 1.30; substrate temperature, 650 °C; laser frequency, 1 Hz; laser power, 200 mJ; O_2 pressure, 3.3 Pa. The distance between the substrate and the target was either 4.5 or 7.5 cm. The deposition rate of the film was about 0.3 nm min^{-1} and the film thickness was around 5–20 nm depending on the duration of the deposition. The $LiCoO_2$ have a layered rock-salt structure (α-$NaFeO_2$ type) with alternating layers of lithium and transition metals, both occupying the octahedral space of a cubic close packed anion array (see Fig. 2). In the space group, R-3m, Li and the transition metal (Co) occupy the 3a and 3b sites, respectively. The disorder at the 3a and 3b sites was estimated from the X-ray intensity ratio of the 0 0 3 and 0 0 6 reflections (I_{003}/I_{006}) for the films of (0 0 l) orientation ($LiCoO_2$ (0 0 3)). Higher O_2 pressure and lower substrate temperature reduced the cation mixing at the 3a and 3b sites, and the film showed more than 90% ordering at these sites. The epitaxial growth was confirmed for all the substrates used in the present study ($SrTiO_3$ (1 1 1), $SrTiO_3$ (1 1 0) and $SrTiO_3$ (1 0 0)). Table 1 summarizes the lattice orientations, lattice parameters and lattice misfit of the deposited

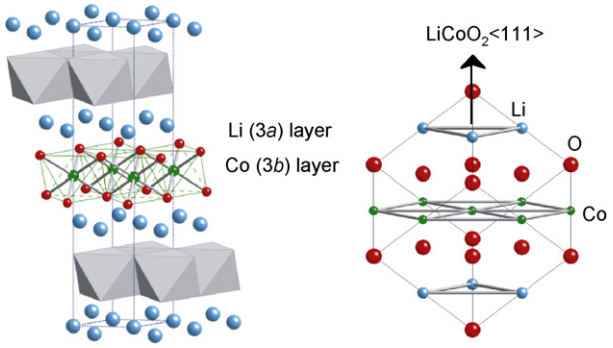

Fig. 2. Structure of $LiCoO_2$ with the layered rock-salt-type (α-$NaFeO_2$).

Table 1
Lattice orientation, lattice parameters and lattice misfit of $LiCoO_2$ thin-films deposited on the $SrTiO_3$ substrates

	$SrTiO_3$ (cubic, a = 3.905Å)		
	(1 1 1)	(1 1 0)	(1 0 0)
$LiCoO_2$ a = 2.81468(3) Å, c = 14.0481(2) Å			
Out-of-plane orientation	0 0 3	1 1 0 (twin crystal)	1 0 4 (twin crystal)
In-plane orientation	$LiCoO_2$ [1 1 0]//$SrTiO_3$ [1 −1 0]	$LiCoO_2$ [0 0 1]//$SrTiO_3$ [1 1 1]	$LiCoO_2$ [1 −2 0]//$SrTiO_3$ [0 1 1]
Lattice parameter	a = 2.8149 Å, c = 14.2234 Å	a = 2.8531 Å, c = 13.8108 Å	a = 2.8126 Å, c = 15.2291 Å
Lattice misfit	1.94%	2.09%	1.86%

Table 2
Relationship between the out-of-plane lattice orientation and two-dimensional layered structure

	Lattice orientation		
	0 0 3	1 1 0	1 0 4
Structure	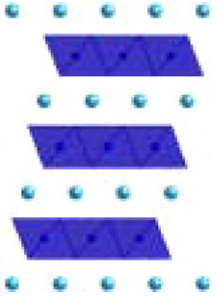	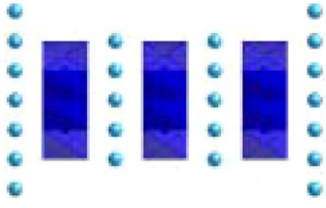	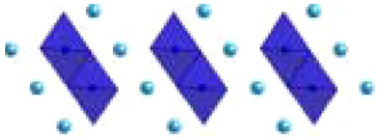

Table 3
Definition of lattice misfit for $LiCoO_2$ deposited on the $SrTiO_3$ substrates

	Definition
Substrate $SrTiO_3$	
(1 1 1)	$f = \frac{d_{f(1\,1\,0)} - d_{s(2\,-2\,0)}}{d_{s(2\,-2\,0)}} \times 100$
(1 1 0)	$f = \frac{d_{f(0\,0\,6)} - d_{s(1\,-1\,1)}}{d_{s(1\,-1\,1)}} \times 100$
(1 0 0)	$f = \frac{d_{f(1\,-2\,0)} - d_{s(0\,2\,2)}}{d_{s(0\,2\,2)}} \times 100$

films on the $SrTiO_3$ substrates. The lattice orientations depend on the lattice-planes of the substrate. Table 2 summarizes lattice orientation of the deposited films together with their schematic drawing of the 2D structure. Table 3 indicates the definition of the lattice misfit. The orientations are described as follows:

$SrTiO_3$ substrate: Fig. 3 shows the XRD patterns of the out-of-plane measurements for $LiCoO_2$ films on the $SrTiO_3$ substrate. The peaks around 43° and 82° were attributed to the reflections of the Fe substrate holder for the XRD measurement. These films have the (0 0 3), (1 1 0) and (1 0 4) orientations on the substrate (1 1 1), (1 1 0) and (1 0 0) planes, respectively. The in-plane XRD was measured along [1 −1 0], [1 −1 1] and [0 1 1] for (1 1 1), (1 1 0) and (1 0 0) planes of the substrates, respectively. The in-plane orientations are summarized as follows:

$SrTiO_3$ (1 1 1): The 1 1 0 reflection of $LiCoO_2$ was observed for the in-plane measurement along [1 −1 0] of the substrate. The rocking curve of the reflection showed a six-fold symmetry, which is consistent with *R*-3*m* symmetry. Fig. 4 shows the reciprocal lattice map around [1 −1 0] of the substrate for $LiCoO_2$ on the $SrTiO_3$ (1 1 1). The 1 1 0 reflection of the deposited film exists close to the 2 −2 0 of the $SrTiO_3$ substrate, indicating epitaxial growth of $LiCoO_2$.

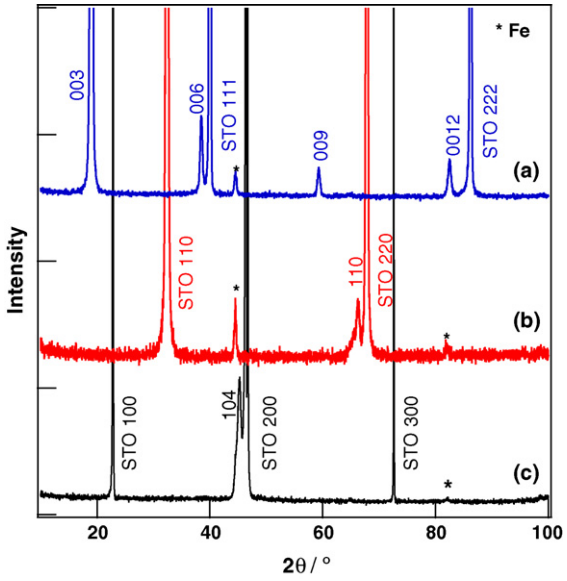

Fig. 3. Out-of-plane X-ray diffraction patterns for $LiCoO_2$ deposited on the $SrTiO_3$ (1 1 1) (a), $SrTiO_3$ (1 1 0) (b) and $SrTiO_3$ (1 0 0) (c) substrates.

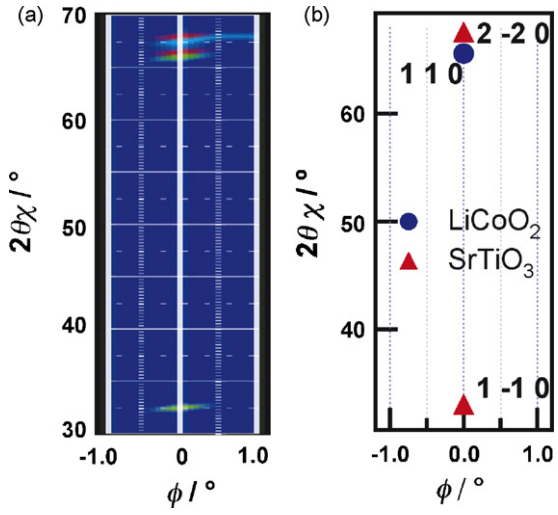

Fig. 4. Reciplocal lattice map of $LiCoO_2$ (0 0 3) deposited on the $SrTiO_3$ (1 1 1) substrate (a). Angle ranges for the measurements are indicated in (b).

$SrTiO_3$ (1 1 0): The in-plane measurement along [1–10] of the substrate indicated 0 0 *l* reflections of $LiCoO_2$. However, the rocking curves of the 0 0 3 reflection showed four-fold symmetry, indicating twin crystal formation with each domain separated by an angle of 70°.

$SrTiO_3$ (1 0 0): The in-plane measurement along [0 1 1] of the substrate indicated (1 −2 0) plane of $LiCoO_2$. The rocking curve of 1 −2 0 reflection showed a four-fold axis, which is

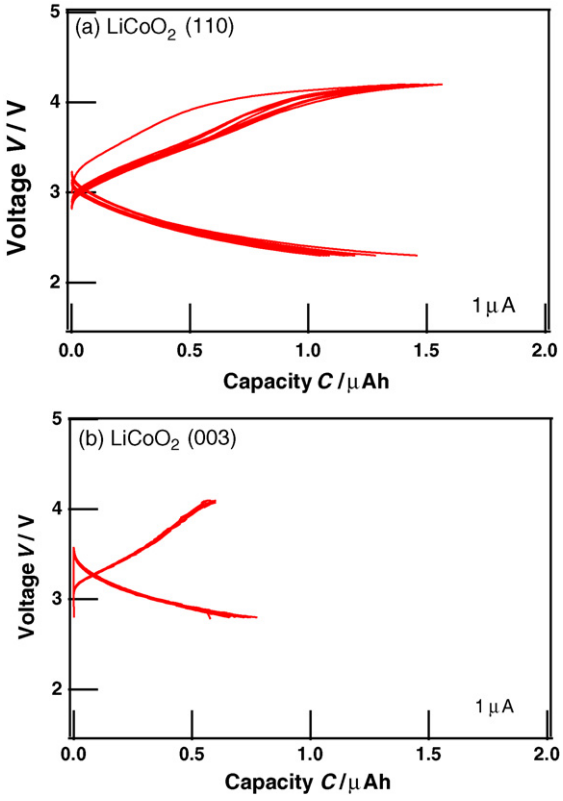

Fig. 5. Charge–discharge curves for the cell using $LiCoO_2$ epitaxial film with the (1 1 0) (a) and (0 0 3) (b) orientations.

indicative of twin crystals with each domain separated by an angle of 90°.

Previously, thin-films of $LiCoO_2$ were synthesized by film deposition techniques under vacuum, such as sputtering and PLD methods on the substrates, Pt, Si or SiO_2 glass [18–21]. While most of these films were polycrystalline state, these films had highly oriented character with (0 0 3) lattice-plane when the film was thin, but changed to random orientations with increasing film-thickness. The random orientation was reported to provide better electrode properties of thin-film lithium batteries. There is another example of the epitaxial film is $LiCoO_2$ with the (0 0 3) orientation synthesized on the MgO substrate by the PLD method [22]. The film had only (0 0 3) orientation and no films with orientation of intercalation active plane were obtained. In the present study, the epitaxial films with different lattice orientations were successfully synthesized for the first time on the $SrTiO_3$ substrates.

3.2. Electrochemical properties of the epitaxial films

Fig. 5 shows the charge–discharge curves of the lithium cells with the epitaxial film electrodes, $LiCoO_2$ (1 1 0) and (0 0 3), deposited on the $SrTiO_3$ (1 1 0) and (1 1 1) substrates, respectively. The $LiCoO_2$ (1 1 0) film showed good reversibility between 2.0 and 4.2 V, while the $LiCoO_2$ (0 0 3) film showed only a limited charge–discharge capacity. The $LiCoO_2$ (0 0 3) film has infinite 2D $[CoO_6]_\infty$ planes face to the electrolyte, while the 2D layer is perpendicular to the electrode/electrolyte interface for $LiCoO_2$ (1 1 0), which allows lithium insertion and extraction from the structure by electrochemical reaction. The charge–discharge behavior of the (1 1 0) and (0 0 3) orientations of the $LiCoO_2$ films is consistent with the structural characteristics.

3.3. Ex situ reflectivity measurements using the epitaxial film electrodes

Fig. 6 shows *ex situ* X-ray reflectivity spectra of the $LiCoO_2$ (1 1 0) (a) and (0 0 3) films (b) with different treatments: the spectra of the as-prepared film (before), after soaked in the electrolyte solution (after) and after setting in the $LiCoO_2$/EC + DEC/Li cell (assemble). All reflectivity spectra are plotted as a function of the scattering vector $q = 4\pi \sin\theta/\lambda$, where λ is the wavelength of the X-ray and θ is the incident angle. The calculated reflectivity curves and the scattering length density (SLD) profiles are also indicated in Fig. 6. Table 4 summarizes the parameters obtained by fitting these data. Three-layers model composed of the $SrTiO_3$ substrate, the $LiCoO_2$ film and a surface layer provided the best fitting of the reflectivity curves for the as-prepared films, $LiCoO_2$ (1 1 0) and (0 0 3). This indicates that the as-grown electrode is covered by an impurity phase with low density, which might be a lithium containing phase, such as lithium carbonate or lithium hydroxide. The SLD profiles of the surface layer also indicate

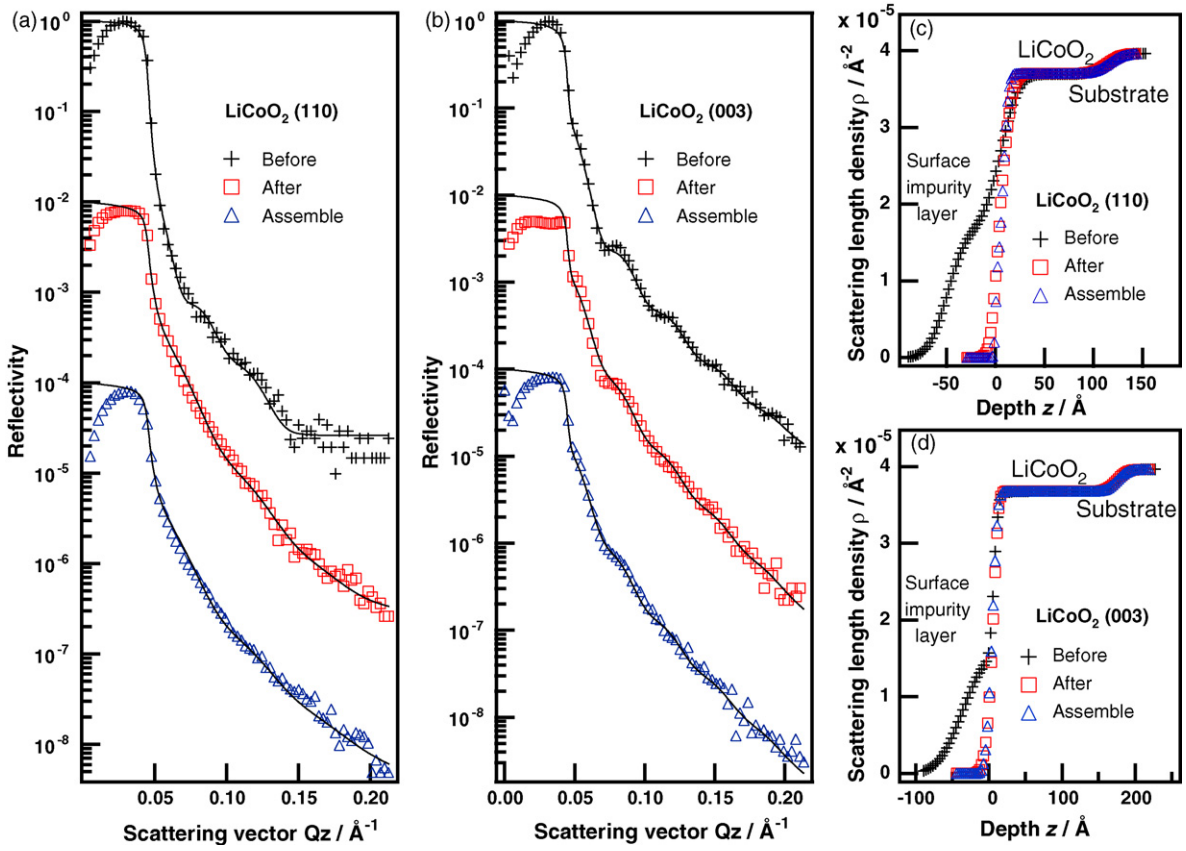

Fig. 6. *Ex situ* X-ray reflectivity spectra (a and b) and scattering length density profiles (c and d) of the $LiCoO_2$ (1 1 0) and $LiCoO_2$ (0 0 3) films with different procedures: the spectra of the film as-prepared (before), after soaked in the electrolyte solution (after) and after setting in the film/EC + DEC/Li cell (assemble).

Table 4
Refined parameters for *ex situ* X-ray reflectivity of $LiCoO_2$ (1 1 0) and $LiCoO_2$ (0 0 3)

	Surface film			$LiCoO_2$			$SrTiO_3$	
	Density d (g cm^{-3})	Thickness l (nm)	Roughness R_s (nm)	Density d (g cm^{-3})	Thickness l (nm)	Roughness R_s (nm)	Density d (g cm^{-3})	Roughness R_s (nm)
(a) $LiCoO_2$ (1 1 0)								
Before	2.11	5.3	1.6	4.67	10.6	1.5	5.15	0.6
After	1.26	0.7	0.5	4.66	10.6	0.8	5.15	0.6
Assemble	1.25	0.8	0.2	4.66	10.6	0.4	5.15	0.6
(b) $LiCoO_2$ (0 0 3)								
Before	1.94	4.2	2.6	4.87	16.7	0.5	5.15	1.1
After	1.94	0.8	0.7	4.87	16.7	0.5	5.15	1.1
Assemble	1.99	0.8	0.5	4.87	16.7	0.5	5.15	1.1

that the film is rather thick and has rough surface. However, the thickness and roughness of the surface layer decreased drastically after the $LiCoO_2$ was soaked into the electrolyte. The film dissolved in the electrolyte.

For the $LiCoO_2$ (0 0 3) electrode, the thickness of the surface layer with a density of 1.9–2.0 decreased from 4.2 nm for the as-grown sample to ~0.8 nm by soaking into the electrolyte. The impurity phase deposited on the surface was dissolved without significant changes in the electrode structures near the surface region of the $LiCoO_2$ (0 0 3) plane. On the other hand, the density of the surface layer deposited on the $LiCoO_2$ (1 1 0) decreased from 2.11 to 1.25 g cm^{-3} after soaking in the electrolyte. The latter value is close to the density of the electrolyte (1.23 g cm^{-3}) EC/DEC (3:7) with $LiPF_6$, which indicates a formation of a new SEI phase originated from the electrolyte composition. The impurity layer was dissolved and the new SEI layer was formed after soaking in the electrolyte at the intercalation active plane (1 1 0).

3.4. *In situ* reflectivity measurements using the epitaxial film electrodes

Fig. 7 shows *in situ* X-ray reflectivity spectra of $LiCoO_2$ (1 1 0) and $LiCoO_2$ (0 0 3) film as a function of cell potential between 2.0 and 4.0 V. No significant changes in the shape of these spectra were detected in the potential range examined. These reflectivity data were then analyzed with a two-layer model where the film was composed of an epitaxial film and a substrate. The potential dependence of the electrode roughness is shown in the same figure. Table 5 summarizes the refined parameters. Although no significant changes were observed in the roughness of the $LiCoO_2$ (0 0 3) electrode (~0.5 nm) between

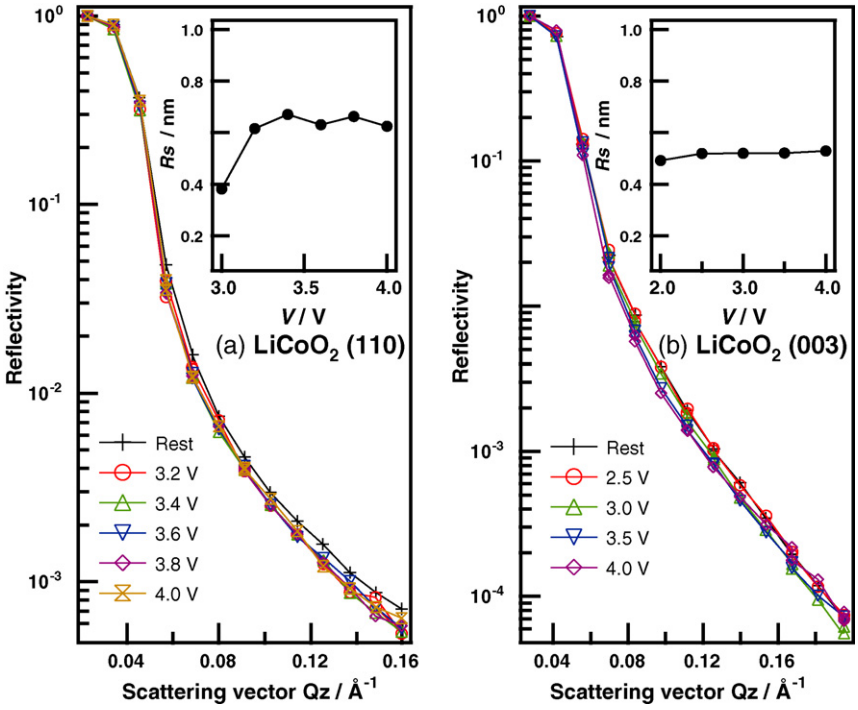

Fig. 7. *In situ* X-ray reflectivity spectra of the epitaxial films of $LiCoO_2$ (1 1 0) (a) and $LiCoO_2$ (0 0 3) (b). The roughness of the electrode surface is indicated as a function of applied potential.

Table 5
Refined parameters for *in situ* X-ray reflectivity of $LiCoO_2$ (1 1 0) and $LiCoO_2$ (0 0 3)

voltage V (V)	$LiCoO_2$			$SrTiO_3$	
	Density d (g cm^{-3})	Thickness l (nm)	Roughness R_s (nm)	Density d (g cm^{-3})	Roughness R_s (nm)
(a) $LiCoO_2$ (1 1 0)					
3.0	5.08	4.9	0.4	5.15	0.5
3.2	5.08	4.9	0.6	5.15	0.5
3.4	5.08	4.9	0.7	5.15	0.5
3.6	5.08	4.9	0.6	5.15	0.5
3.8	5.08	4.9	0.7	5.15	0.5
4.0	5.08	4.9	0.6	5.15	0.5
3.0	5.08	4.9	0.7	5.15	0.5
(b) $LiCoO_2$ (0 0 3)					
2.0	5.08	9.0	0.5	5.15	0.5
2.5	5.08	9.0	0.5	5.15	0.5
3.0	5.08	9.0	0.5	5.15	0.5
3.5	5.08	9.0	0.5	5.15	0.5
4.0	5.08	9.0	0.5	5.15	0.5
1.7	5.08	9.0	0.4	5.15	0.5

3.0 and 4.0 V, the $LiCoO_2$ (1 1 0) film showed a slight increase in the roughness from 0.4 to 0.7 nm with applying voltage from 3.0 to 3.2 V and became constant between 3.2 and 4.0 V. The intercalation active plane of $LiCoO_2$ (1 1 0) composed of the 2D edge has slightly larger surface roughness than the non-intercalation plane $LiCoO_2$ (0 0 3). The intercalation reaction through the (1 1 0) surface may affect the $LiCoO_2$ electrode structure. On the other hand, no SEI phase was observed on the $LiCoO_2$ (1 1 0) during the first charge cycling, as the density of the SEI layer detected by the *ex situ* measurements is close to that of the electrolyte. Fig. 8 shows the AFM images of $LiCoO_2$ (1 1 0) and (0 0 3) films before and after the *in situ* X-ray reflectivity measurements. No changes in morphology were observed for the $LiCoO_2$ films after the electrochemical test. As the AFM observes the surface of the electrode including SEI layer, these results are consistent with the small roughness of the SEI layer for both (0 0 3) and (1 1 0) planes observed by the reflectivity measurements.

The results obtained by *ex situ* and *in situ* X-ray reflectivity and AFM measurements are summarized as follows.

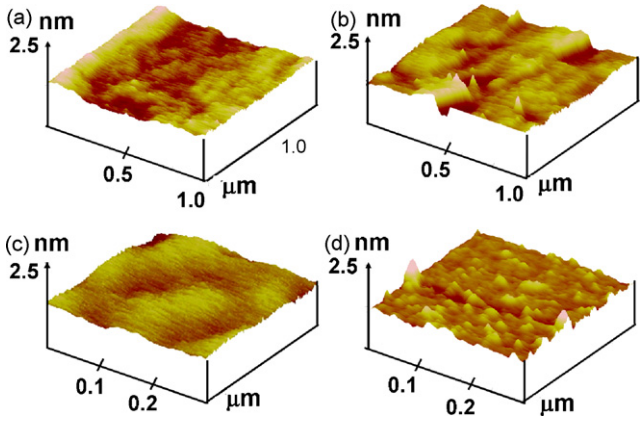

Fig. 8. AFM images of the $LiCoO_2$ films deposited with a laser power of 100 mJ: (1 1 0) (a) and (0 0 3) (b) orientations. AFM images of $LiCoO_2$ after the *in situ* X-ray reflectivity measurements. (1 1 0) (c) and (0 0 3) (d) orientations.

(i) An additional surface layer was observed for the as-grown $LiCoO_2$ film. The film was estimated from its density to be lithium containing materials, such as lithium carbonate, and dissolved after the $LiCoO_2$ was soaked into the electrolyte. The new SEI phase was observed only on the intercalation active plane, $LiCoO_2$ (1 1 0) after soaking into the electrolyte, while the $LiCoO_2$ (0 0 3) surface remained unchanged.
(ii) *In situ* X-ray reflectivity indicated that the surface roughness for the intercalation plane of $LiCoO_2$ (1 1 0) increased with applying cell voltages. The $LiCoO_2$ (1 1 0) showed slightly larger surface roughness than the $LiCoO_2$ (0 0 3) during the electrochemical reaction. The intercalation reaction caused a surface structure change of $LiCoO_2$.
(iii) The AFM observation showed no significant changes in the surface morphology for $LiCoO_2$ (1 1 0) and $LiCoO_2$ (0 0 3) after the electrochemical reaction, as the AFM technique observes the surface of the SEI layer on the electrode surface.

Recent *ex situ* spectroscopic studies on polycrystalline cathode materials, $LiCo_{0.2}Ni_{0.8}O_2$ and $LiMn_2O_4$, indicated that a SEI phase was formed after charge–discharge cycling, and that the phase was composed of multi-layers with inorganic and organic components [5–12]. The measurements using polycrystalline materials could not assign the anisotropy of interfacial reactions. On the other hand, our results obtained by the *ex situ* X-ray reflectivity indicated that the SEI phase was formed at the very beginning of the reaction by soaking into the electrolyte only on the intercalation plane, $LiCoO_2$ (1 1 0). Furthermore, the electrode surface was affected by the intercalation reaction; the surface roughness of the (1 1 0) plane increased. These results suggest that the surface atomic arrangements were significantly disturbed by the intercalation reactions. Further studies on surface X-ray diffraction to clarify the atomic arrangements near the electrode surface are currently underway.

In the present study, the experimental technique using X-ray reflectivity and epitaxial thin-film electrodes was applied for lithium-ion battery at the first time. We could successfully detect the changes at the first step of the interfacial reaction between the electrode and the electrolyte and clarify an anisotropic reactivity due to the orientations of the electrode.

4. Summary

We developed the experimental technique using epitaxial thin-film electrodes and X-ray reflectometry for detecting structure changes at electrode/electrolyte interface in lithium-ion batteries. The lattice orientations of $LiCoO_2$ with the layered roc-ksalt structure are characterized by thin-film XRD. The $LiCoO_2$ films have a 2D transition metal layer parallel and perpendicular to the substrates depending on the substrate orientation. The thickness of these films was 5–17 nm. The electrochemical properties of these films showed anisotropic properties depending on the film orientations. The electrochemical characterization of these films revealed that the $LiCoO_2$ (0 0 3) showed only a limited capacity, while the $LiCoO_2$ (1 1 0) showed reversible electrode reaction, which is consistent with a structure consideration that the active intercalation sites situate on the edge planes of the 2D layered structure. The X-ray reflectivity study at the electrode/electrolyte interface indicated the orientation dependence of the morphology changes. Our new methods of surface reflectivity using an epitaxial film electrode are promising technique to elucidate the interfacial reactions at the electrode/electrolyte interface for lithium batteries.

Acknowledgements

The present work was carried out as a collaboration program with the Genesis Research Institute. This work was partly supported by the Grant-in-Aid for Scientific Research (A), Japan Society for the Promotion of Science.

References

[1] K. Mizushima, P.C. Jones, P.J. Wiseman, J.B. Goodenough, Mater. Res. Bull. 15 (6) (1980) 783–789;
JP, 62-23433, B (1987);
R. Kanno, Y. Takeda, T. Ichikawa, K. Nakanishi, O. Yamamoto, J. Power Sources 26 (3/4) (1989) 535;
M. Mohri, N. Yanagisawa, Y. Tajima, H. Tanaka, T. Mitate, S. Nakajima, M. Yoshida, Y. Yoshimoto, T. Suzuki, H. Wada, J. Power Sources 26 (3/4) (1989) 545.
[2] T. Abe, H. Fukuda, Y. Iriyama, Z. Ogumi, J. Electrochem. Soc. 151 (2004) A1120.
[3] Z. Ogumi, T. Abe, T. Fukutsuka, S. Yamate, Y. Iriyama, J. Power Sources 127 (2004) 72.
[4] E. Peled, J. Electrochem. Soc. 126 (1979) 2047.
[5] M.S. Wu, P.C.J. Chiang, J.C. Lin, J. Electrochem. Soc. 152 (2005) A1041.
[6] A. Schechter, D. Aurbach, H. Cohen, Langmuir 15 (1999) 3334.
[7] D. Bar-Tow, E. Peled, L. Burstein, J. Electrochem. Soc. 146 (1999) 824.
[8] K. Araki, N. Sato, J. Power Sources 124 (2003) 124.
[9] D. Aurbach, K. Gamolsky, B. Markovsky, G. Salitra, Y. Gofer, U. Heider, R. Oesten, M. Schmidt, J. Electrochem. Soc. 147 (2000) 1322.
[10] D. Aurbach, M.D. Levi, E. Levi, H. Teller, B. Markovsky, G. Salitra, U. Heider, L. Heider, J. Electrochem. Soc. 145 (1998) 3024.
[11] M. Menetrier, C. Vaysse, L. Croguennec, C. Delmas, C. Jordy, F. Bonhomme, P. Biensan, Electrochem. Solid State Lett. 7 (2004) A140.
[12] J.L. Lei, L.J. Li, R. Kostecki, R. Muller, F. McLarnon, J. Electrochem. Soc. 152 (2005) A774.
[13] M.G. Samant, M.F. Toney, G.L. Borges, L. Blum, O.R. Melroy, Surf. Sci. Lett. 193 (1988) L29–L36.
[14] B.M. Ocko, J. Wang, Phys. Rev. Lett. 65 (1990) 1466.
[15] Z. Nagy, H. You, R.M. Yonco, C.A. Melendres, W. Yun, V.A. Maroni, Electrochm. Acta 36 (1991) 209.
[16] L.G. Parratt, Phys. Rev. 95 (1954) 359.
[17] C. Braun, The Reflectivity Tool or Parratt32 Version 1.6.0, HMI, Berlin, 1997–2002.
[18] J.B. Bates, N.J. Dudney, ASAIO J. 43 (1997) M644.
[19] C. Julien, M.A. Camacho-Lopez, L. Escobar-Alarcon, E. Haro-Poniatowski, Mater. Chem. Phys. 68 (2001) 210.
[20] B.J. Neudecker, N.J. Dudney, J.B. Bates, J. Electrochem. Soc. 147 (2000) 517.
[21] B.J. Neudecker, R.A. Zuhr, J.B. Bates, J. Power Sources 82 (1999) 27.
[22] M. Morcrette, A. Gutierrex-Llorente, W. Seiler, J. Perriere, A. Laurent, P. Barboux, J. Appl. Phys. 88 (9) (2000) 5100.